

Nucleation-type magnetization behavior in FePt (001) particulate films

T. Shima^{a)} and K. Takanashi

Institute for Materials Research, Tohoku University, Sendai 980-8577, Japan

Y. K. Takahashi and K. Hono

National Institute for Materials Science, Tsukuba 305-0047, Japan

G. Q. Li and S. Ishio

Venture Business Laboratory, Akita University, Akita 010-8502, Japan

(Received 7 April 2005; accepted 21 December 2005; published online 10 February 2006)

Nucleation-type magnetization behavior is reported in sputtered FePt (001) films with an island structure, where the particles show a multiple-domain structure. A large coercivity H_C of more than 50 kOe is achieved at an initial applied field of only 6 kOe. The magnetization behavior and the magnetic domain observation indicate clearly that domain walls are wiped out completely at a low applied field, and once domain walls are wiped out, it is hard to nucleate reversed domains in the particles, resulting in high H_C . The remarkable nucleation-type behavior of magnetization is also found to give rise to anomalous minor loops when the applied magnetic field is alternated around zero and increased gradually. © 2006 American Institute of Physics. [DOI: 10.1063/1.2169878]

I. INTRODUCTION

The technical magnetization process of hard magnets, i.e., the materials with high magnetic anisotropy, has been investigated for a long time,^{1,2} and it is generally classified into two types: the nucleation type, where the coercive force H_C is dominated by the nucleation of reversed domains as observed for NdFeB-type magnets, and the pinning type, where H_C is dominated by the pinning of domain walls as observed for Sm₂Co₁₇-type magnets.³ Not only in pinning-type but also in nucleation-type magnets, an initial applied field H_s required to fully magnetize the material to obtain sufficiently high H_c is usually comparable to H_c , although the origins for H_s and H_c arise from different physical phenomena in nucleation-type magnets. Recently, $L1_0$ -ordered FePt alloy with high magnetocrystalline anisotropy ($K_u = 7.0 \times 10^7$ ergs/cc) has attracted much attention,⁴⁻²² since they are believed to be good candidates for future magnetic devices such as next-generation ultrahigh-density magnetic storage media and biasing nanomagnets. Therefore, a lot of studies have focused on the fabrication of $L1_0$ -ordered FePt thin films by conventional deposition techniques⁴⁻²¹ and of nanoparticles by chemical synthesis.²² However, the magnetization process for highly coercive FePt films has not fully been investigated to date. Previously, we reported that a high coercivity of 70 kOe was successfully achieved at room temperature for FePt particulate films sputtered on MgO (001) substrates.²¹ These films had epitaxially grown a highly $L1_0$ -ordered structure. In this paper, we demonstrate a remarkable nucleation-type behavior of magnetization showing $H_s \ll H_c$, in an assembly of almost defect-free and perfectly aligned FePt nanoparticles with a multiple-domain structure.

II. EXPERIMENTAL PROCEDURE

The samples were prepared by cosputtering Fe and Pt directly onto single-crystal MgO (100) substrates using an UHV-compatible dc-sputtering apparatus (base pressure of $\sim 5 \times 10^{-10}$ Torr). The targets were commercial products with purities higher than 99.99 at. % for Fe and 99.9 at. % for Pt. The typical growth rate for FePt was 0.12 nm/s. The substrates were attached to a rotating table and heated up to 780 °C during the deposition. The compositions of deposited films were determined to be Fe₅₂Pt₄₈ by electron probe x-ray microanalysis (EPMA). The morphology of the FePt films was controlled by varying the nominal thickness (t_N).¹⁵ In this work t_N was varied in the range of 1–40 nm, where the films show an island growth and the average particle size increases with t_N . The structural analysis was performed by transmission electron microscopy (TEM) and x-ray diffraction (XRD) with Cu $K\alpha$ radiation. Magnetization curves were measured by a superconducting quantum interference device (SQUID) magnetometer, and in some cases, a vibrating sample magnetometer (VSM) equipped with a superconducting magnet (maximum magnetic field of ± 140 kOe) at temperatures of 4.5 and 295 K was used. The magnetic domain structure was observed by magnetic force microscopy (MFM) in applied fields up to ± 6 kOe.

III. RESULTS AND DISCUSSION

The FePt nanoparticles were epitaxially grown with the cube-cube orientation relationship with the MgO substrate, showing the c axis perpendicular to the substrate plane. For example, Fig. 1 shows TEM images for $t_N = 20$ nm. The distribution of particle sizes is bimodal, consisting of larger ones with the typical size of about a few hundreds of nanometers and smaller ones with {001} faceted morphology whose size ranges from 10 to 50 nm in side [Fig. 1(a)]. The heights of large particles are almost the same (~ 25 nm) with a perfectly flat (100) surface with small {001} facets, as seen

^{a)} Author to whom correspondence should be addressed; present address: Department of Applied Physics and Informatics, Tohoku-Gakuin University; electronic mail: shima@imr.tohoku.ac.jp

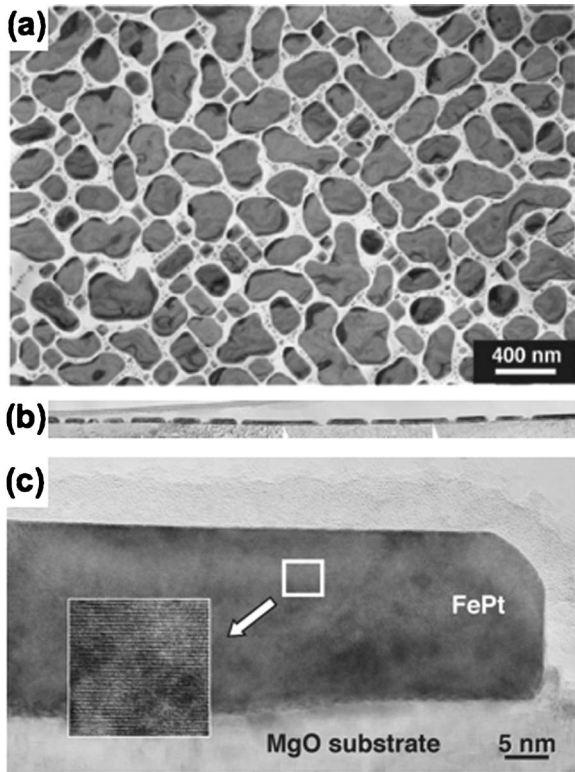


FIG. 1. TEM images of a FePt film with nominal thickness $t_N=20$ nm. In-plane bright field image (a), cross-sectional image (b), and high-resolution cross-sectional image (c).

from the cross-sectional image [Fig. 1(b)]. The enlarged cross-sectional image clearly shows the contrast corresponding to the alternate stacking of Fe and Pt monatomic layers in the [001] direction of the $L1_0$ -ordered structure [Fig. 1(c)]. Although these large particles are formed by the coalescence of small particles, no structural defects such as twins can be seen and the surfaces of particles are atomically flat, indicating the formation of defect-free, perfectly aligned, single-crystalline FePt nanoparticles.

Figure 2 shows H_C as a function of t_N at room temperature [Fig. 2(a)] and at 4.5 K [Fig. 2(b)]. H_C was obtained from the magnetization curves measured with the applied magnetic field perpendicular to the substrate plane using a

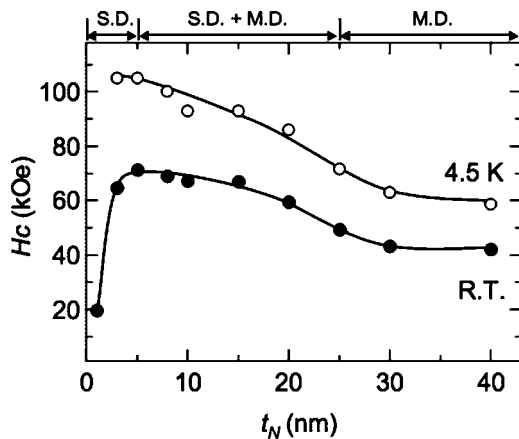


FIG. 2. Coercivity H_C as a function of nominal thickness t_N at room temperature and 4.5 K. The lines are guides to the eye.

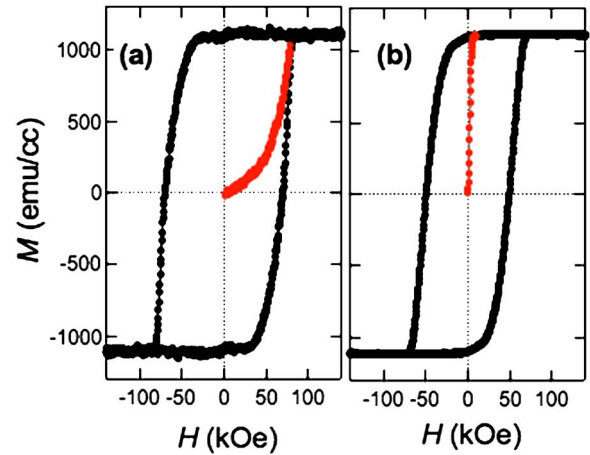


FIG. 3. (Color online) Magnetization curves of FePt films with nominal thicknesses $t_N=5$ nm (a) and 25 nm (b). Initial magnetization curves are also indicated. The difference between the magnetization processes in single-domain (SD) and multiple-domain (MD) particles is clearly demonstrated.

VSM equipped with a superconducting magnet. Huge H_C values of 70 kOe at room temperature and of 105 kOe at 4.5 K were obtained for $t_N=5$ nm.²¹ Both at room temperature and at 4.5 K, H_C decreases gradually with t_N . However, H_C keeps large values (42 and 59 kOe at room temperature and at 4.5 K, respectively), even for $t_N=40$ nm. It has been found from MFM observation¹⁷ that most of the particles have the single-domain (SD) state for $t_N \leq 5$ nm, where the particle sizes are a few tens of nanometers or smaller. A rapid decrease of H_C for $t_N \leq 3$ nm at room temperature is caused by poor chemical order in small particles with diameters less than a few nanometers.^{19,20} As t_N increases, multiple-domain (MD) particles appear with increasing average size, and most of the particles have the MD state for $t_N \geq 25$ nm, where the particle sizes are typically of the order of hundred of nanometers. SD and MD particles are mixed in the intermediate region between $t_N=5$ and 25 nm. The difference between the magnetization processes in SD and MD particles is clearly demonstrated by the initial magnetization curves starting from the demagnetized state. For the SD particles, the initial magnetization increases slowly with the applied magnetic field and becomes hard to saturate [Fig. 3(a)], indicating that the magnetization process is dominated by magnetization rotation, which is mostly incoherent rather than coherent. The very same processes determine the magnetization variation in the initial state (red curve in Fig. 3) and after saturation (hysteresis cycle in black). For the MD particles, on the other hand, the initial magnetization increases steeply and saturates easily [Fig. 3(b)], indicating that the magnetization process is dominated by domain-wall displacement. In other words, a typical nucleation-type behavior of magnetization is observed in the MD particles.

It is well known that usually a high magnetic field comparable to H_C is required to fully magnetize hard magnetic materials even in the case of the “nucleation-type” magnetization process.²³ In other words, a high magnetic field comparable to H_C is required to wipe out domain walls completely to obtain sufficiently high H_C . However, the FePt nanoparticles studied in this paper are clearly different. Fig-

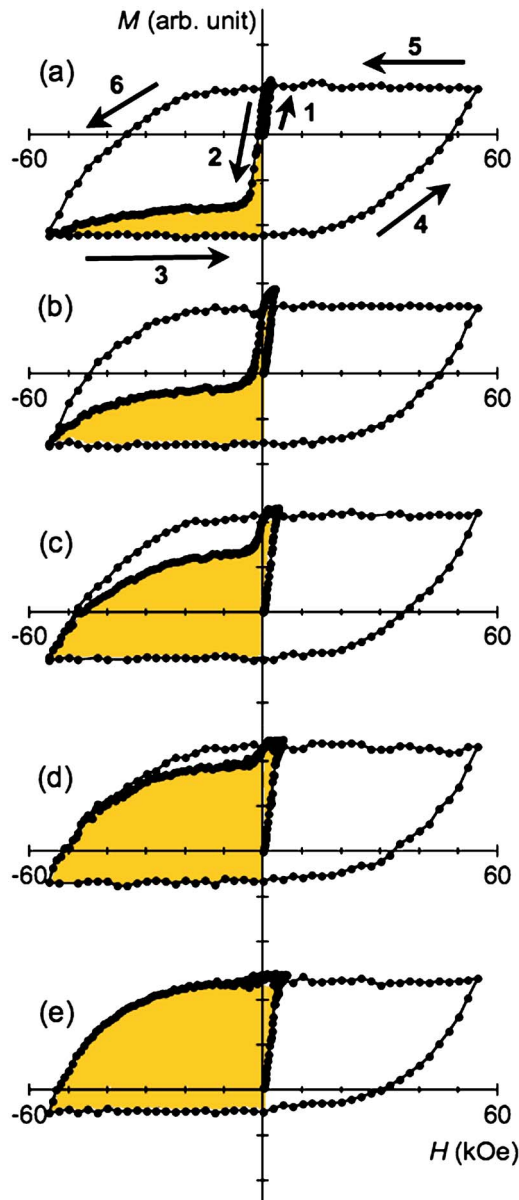


FIG. 4. (Color online) Magnetization curves for nominal thickness $t_N = 25$ nm, with the varying initial applied field (H_{in}) from the virgin state. H_{in} is 2 kOe (a), 3 kOe (b), 4 kOe (c), 5 kOe (d), and 6 kOe (e). The magnetic field is first increased to $H_{in} = +2$ kOe from the virgin state (arrow 1), then reversed to -55 kOe (arrow 2), again increased through zero to $+55$ kOe (arrows 3 and 4), and reversed again through zero to -55 kOe (arrows 5 and 6).

ure 4 shows the magnetization curves for $t_N = 25$ nm with various initial applied fields ($H_{in} = 2, 3, 4, 5,$ and 6 kOe) from the virgin state. In the case of $H_{in} = 2$ kOe [Fig. 4(a)], most of the particles reverse the magnetization easily at low magnetic fields of a few Kilo-oersted when the magnetic field is reversed [arrow 2 in Fig. 4(a)]. With increasing H_{in} , the fraction of the particles showing easily reversed magnetization decreases [Figs. 4(b)–4(d)], and finally it disappears at $H_{in} = 6$ kOe [Fig. 4(e)]. This result indicates that only 6 kOe is enough to fully magnetize the sample to obtain a high H_C value of more than 50 kOe. In other words, domain walls are wiped out completely from each particle at a low magnetic field. Then, it becomes very hard to nucleate reversed domains; a high magnetic field becomes necessary for a mag-

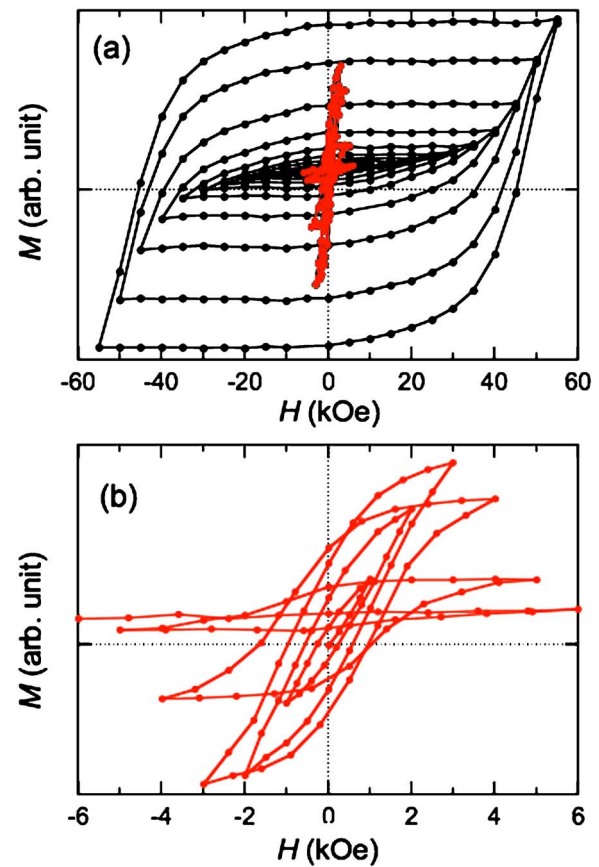


FIG. 5. (Color online) Magnetization curves including minor loops with the increasing maximum applied fields H_{max} . Minor loops for a FePt film with nominal thickness $t_N = 25$ nm as H_{max} is increased from 1 to 55 kOe gradually (a) and enlarged minor loops at a small magnetic-field region (b) which is marked in (a).

netization reversal. This remarkable nucleation-type behavior is caused by two possible origins: one is the ideal structure with defect-free, perfectly aligned, monocrystalline FePt nanoparticles, leading to a free domain-wall movement, and the other is the reduced dipolar interaction between FePt nanoparticles due to larger interparticle distances than those in sintered bulk magnets.^{24–26} As seen from the cross-sectional TEM image, the particles are fully ordered to the terminal surface layer of the particle, so no low K_u region is expected at the surface, unlike imperfect grain boundaries of $Nd_2Fe_{14}B$ sintered magnets.

We find that the nucleation-type behavior leads to anomalous minor loops when they are measured upon increasing the maximum applied field H_{max} gradually. The minor loop is the magnetic hysteresis loop measured with the applied field that is lower than the saturation field. Starting from the virgin demagnetized state, the magnetization of minor loops usually increases with H_{max} . The minor loops for the sample with $t_N = 25$ nm are shown in Figs. 5(a) and 5(b) with gradually increasing H_{max} from 1 to 50 kOe. When H_{max} is small (≤ 3 kOe), the magnetization increases with H_{max} . When H_{max} exceeds 3 kOe, however, the magnetization starts to decrease with H_{max} , showing a clear contrast to the general expectation. The magnetization becomes a small constant value independent of the applied field for $H_{max} = 6$ kOe [Fig.

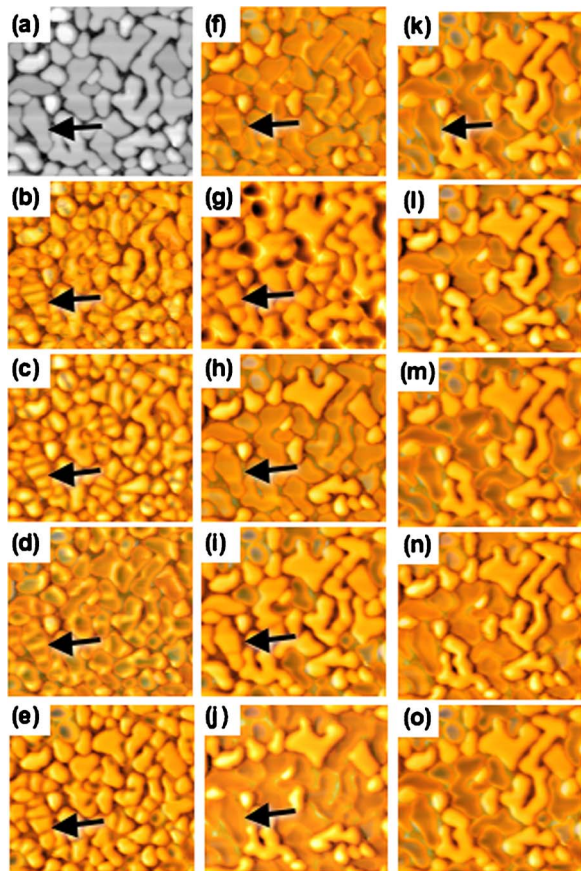


FIG. 6. (Color online) Atomic force microscopy (AFM) images (a) and magnetic force microscopy (MFM) images superimposed with AFM images [(b)–(o)] for a FePt film with $t_N=25$ nm, when the applied magnetic field is alternated around zero and increased gradually. Applied magnetic fields are (b) 0 (virgin state), (c) +1 kOe (d) –1 kOe, (e) +2 kOe, (f) –2 kOe, (g) +3 kOe, (h) –3 kOe, (i) +4 kOe, (j) –4 kOe, (k) +5 kOe, (l) –5 kOe, (m) +6 kOe, (n) –6 kOe, and (o) +10 kOe.

5(b)]. The almost constant magnetization is maintained until H_{\max} reaches 20 kOe, and the magnetization starts to increase again for $H_{\max} \geq 20$ kOe.

This anomalous behavior of the minor loops is explained as follows: In the minor loops with small maximum fields, the fraction of domains with the same direction as the applied field increases with the applied field due to the domain-wall displacement in MD particles. Therefore, the magnetization normally increases with H_{\max} . When domain walls are wiped out from a particle and the particle becomes SD by increasing H_{\max} , the magnetization direction of the particle does not change until H_{\max} exceeds a nucleation field. Because the minor loops are measured by alternating the applied field before the magnetization direction are completely aligned to one direction, the magnetization vectors of some particles are upward and those of other particles are downward, resulting in a lower value than the saturation magnetization. We can actually see the magnetic domain structure and the transition from the MD to the SD state in a particle by a MFM observation in applied fields. Figure 6 shows MFM images superimposed with atomic force microscopy (AFM) images when the applied magnetic field is alternated around zero and increased gradually. In the virgin state [$H_{\text{in}}=0$ kOe, Fig. 6(b)], contrasting bright and dark regions

corresponding to the magnetization directions upward and downward, respectively, are clearly seen in a particle, showing the MD state. When a magnetic field of 1 kOe is applied in the upward direction ($H_{\text{in}}=+1$ kOe; the positive sign is defined as the upward direction), the bright region corresponding to the domains with an upward magnetization is expanded and the dark region corresponding to the domains with a downward magnetization shrinks [Fig. 6(c)]. When the magnetic field is reversed $H_{\text{in}}=-1$ kOe; on the other hand, the dark region is expanded and the bright region shrinks [Fig. 6(d)]. Now let us take a closer look at the particle indicated by the arrow. The number of bright and dark stripes in the particle corresponds to that of domains. The number of domains in the particle decreases gradually with the increasing applied field [$H_{\text{in}} < +4$ kOe, Figs. 6(c)–6(i)], and finally the particle entirely turns dark at $H_{\text{in}}=-4$ kOe [Fig. 6(j)]. In other words, the MD particle changes into a SD particle with a downward magnetization. Likewise, another particle changes into a SD particle with an upward magnetization. Consequently, the sample consists of SD particles with upward and downward magnetization directions. For $H_{\text{in}} \geq +5$ kOe or $H_{\text{in}} \leq -5$ kOe, no change in MFM images is seen, indicating that each particle keeps the same magnetization direction [Figs. 6(k)–6(o)]. The unsaturated sample containing upward and downward magnetization vectors gives a lower magnetization, which is the difference between the fractions of the upward and downward particles.

IV. CONCLUSION

The present study has demonstrated the nucleation-type behavior of magnetization: a large H_C of more than 50 kOe is achieved at an initial applied field of only 6 kOe in FePt nanoparticles with a multiple-domain structure. The magnetization behavior and the magnetic domain observation indicate clearly that domain walls are wiped out completely at a low applied field. Once domain walls are wiped out, the nucleation of the reversed domains becomes difficult in the particles, resulting in high H_C . A smooth displacement of unpinned domain walls and high nucleation field values of reversed domains are essential for the remarkable nucleation-type behavior. These which are associated with the ideal structure of defect-free and perfectly aligned FePt nanoparticles that are epitaxially grown on MgO single-crystal substrates. In addition, the dipolar interaction between neighboring particles is thought to be reduced in this island structure, compared to that in well-known sintered bulk magnets. We have also found that the nucleation-type behavior leads to anomalous minor loops when they are measured upon increasing the maximum applied field H_{\max} gradually. Although the assembly of MD particles with a high H_C is not suitable for rewritable ultrahigh-density magnetic recording media, this type of film may be useful as an “eternal” magnetic recording media, which are easily magnetized at a low magnetic field using the existing magnetic recording heads for writing but are hardly demagnetized by any environmental disturbance such as oxidation, thermal agitation, and external magnetic field. Although the bit information of the present high-density magnetic recording media is thought to

become unstable only after ten years, the easily magnetized but hardly demagnetized films can maintain the information once they are written at a low magnetic field.

ACKNOWLEDGMENTS

We thank J. A. C. Bland for a critical reading of this manuscript, S. Sugimoto for a fruitful discussion, and Y. Murakami for his technical assistance. This work was partly supported by the Special Coordination Funds for Promoting Science and Technology on “Nanohetero Metallic Materials” from the Ministry of Education, Culture, Sports, Science and Technology. X-ray-diffraction measurements were performed at the Laboratory for Advanced Materials, IMR, Tohoku University. High-field magnetic measurements were performed at the Center for Low Temperature Science, Tohoku University.

¹C. Kittel, *Phys. Rev.* **70**, 965 (1946).

²E. C. Stoner and E. P. Wohlfarth, *Philos. Trans. R. Soc. London, Ser. A* **240**, 599 (1948).

³É. du Trémolet de Lacheisserie, D. Gignoux, and M. Schlenker, *Magnetism; Fundamentals* (Kluwer Academic Group, Dordrecht, 2002), Vol. I, pp. 234–235.

⁴B. M. Lairson, M. R. Viosokay, R. Sinclair, and B. M. Clemens, *Appl. Phys. Lett.* **62**, 639 (1993).

⁵A. Cebollada, D. Weller, J. Sticht, G. R. Harp, R. F. C. Farrow, R. F. Marks, R. Savoy, and J. C. Scott, *Phys. Rev. B* **50**, 3419 (1994).

⁶M. Watanabe and M. Homma, *Jpn. J. Appl. Phys., Part 2* **35**, L1264 (1996).

⁷Y. Ide, T. Goto, K. Kikuchi, K. Watanabe, J. Onagawa, H. Yoshida, and J. M. Cadogan, *J. Magn. Magn. Mater.* **177–181**, 1245 (1998).

⁸T. Suzuki, K. Harada, N. Honda, and K. Ouchi, *J. Magn. Magn. Mater.* **193**, 85 (1999).

⁹D. Weller *et al.*, *IEEE Trans. Magn.* **36**, 10 (2000).

¹⁰D. Ravelosona, C. Chappert, V. Mathet, and H. Bernas, *J. Appl. Phys.* **87**, 5771 (2000).

¹¹Y. Endo, N. Kikuchi, O. Kitakami, and Y. Shimada, *J. Appl. Phys.* **89**, 7065 (2001).

¹²Y.-N. Hsu, S. Jeong, D. E. Laughlin, and D. N. Lambeth, *J. Appl. Phys.* **89**, 7068 (2001).

¹³T. Maeda, T. Kai, A. Kikitsu, T. Nagase, and J. Akiyama, *Appl. Phys. Lett.* **80**, 2147 (2002).

¹⁴T. Shima, T. Moriguchi, S. Mitani, and K. Takanashi, *Appl. Phys. Lett.* **80**, 288 (2002).

¹⁵T. Shima, K. Takanashi, Y. K. Takahashi, and K. Hono, *Appl. Phys. Lett.* **81**, 1050 (2002).

¹⁶T. Seki, T. Shima, K. Takanashi, Y. Takahashi, E. Matsubara, and K. Hono, *Appl. Phys. Lett.* **82**, 2461 (2003).

¹⁷G. Q. Li, H. Takahashi, H. Ito, H. Saito, S. Ishio, T. Shima, and K. Takanashi, *J. Appl. Phys.* **94**, 5672 (2003).

¹⁸S. Okamoto, O. Kitakami, N. Kikuchi, T. Miyazaki, Y. Shimada, and Y. K. Takahashi, *Phys. Rev. B* **67** 094422 (2003).

¹⁹Y. K. Takahashi, T. Ohkubo, M. Ohnuma, and K. Hono, *J. Appl. Phys.* **93**, 7166 (2003).

²⁰Y. K. Takahashi, T. Koyama, M. Ohnuma, T. Ohkubo, and K. Hono, *J. Appl. Phys.* **95**, 2690 (2004).

²¹T. Shima, K. Takanashi, Y. K. Takahashi, and K. Hono, *Appl. Phys. Lett.* **85**, 2571 (2004).

²²S. Sun, C. B. Murray, D. Weller, L. Folks, and A. Moser, *Science* **287**, 1989 (2000).

²³D. W. Taylor, V. Villas-Boas, Q. Lu, M. F. Rossignol, F. P. Missell, D. Givord, and S. Hirose, *J. Magn. Magn. Mater.* **130**, 225 (1994).

²⁴K.-D. Durst and H. Kronmüller, *J. Magn. Magn. Mater.* **68**, 63 (1987).

²⁵D. Givord, P. Tenaud, and T. Viadieu, *IEEE Trans. Magn.* **24**, 1921 (1988).

²⁶D. Givord, Q. Lu, F. P. Missell, M. F. Rossignol, D. W. Taylor, and V. Villas Boas, *J. Magn. Magn. Mater.* **104–107**, 1129 (1992).